ACTIVE TWIST OF MODEL ROTOR BLADES WITH D-SPAR DESIGN

Andrejs Kovalovs [1], Evgeny Barkanov [2], Sergejs Gluhihs [3]

Institute of Materials and Structures, Riga Technical University, Azenes st. 16-323, LV-1048 Riga, Latvia
E-mails: [1]kovalovs@bf.rtu.lv; [2]barkanov@latnet.lv; [3]s_gluhih@inbox.lv

Abstract. The design methodology based on the planning of experiments and response surface technique has been developed for an optimum placement of Macro Fiber Composite (MFC) actuators in the helicopter rotor blades. The baseline helicopter rotor blade consists of D-spar made of UD GFRP, skin made of $+45^0/-45^0$ GFRP, foam core, MFC actuators placement on the skin and balance weight. 3D finite element model of the rotor blade has been built by ANSYS, where the rotor blade skin and spar "moustaches" are modeled by the linear layered structural shell elements SHELL99, and the spar and foam - by 3D 20-node structural solid elements SOLID186. The thermal analyses of 3D finite element model have been developed to investigate an active twist of the helicopter rotor blade. Strain analogy between piezoelectric strains and thermally induced strains is used to model piezoelectric effects. The optimisation results have been obtained for design solutions, connected with the application of active materials, and checked by the finite element calculations.

Keywords: active twist, Macro Fiber Composite (MFC), helicopter rotor blade, optimal design, finite element method.

1. Introduction

In time of helicopter flight rotor blades produce significant vibration and noise as a result of variations in rotor blade aerodynamic loads with blade azimuth angle. For this reason future helicopters need to be improved with respect to environmental and public acceptance. Significant vibration and noise reduction can be achieved without the need for complex mechanisms in the rotating system using active twist control of helicopter rotor blades by the application of MFC actuators. In this case MFC actuators are implemented in the form of active plies within the composite skin of the rotor blade with orientation at 45^0 to the blade axis to maximize the shear deformations in the laminated skin producing a distributed twisting moment along the blade.

A number of theoretical and experimental studies have been performed to estimate an active twist of helicopter rotor blades required to effect noise and vibration reduction benefits, as well as to improve the overall performance of helicopters [1–4]. The design of an active blade model based on a 1/6th Mach-scale Chinook CH-47D has been reviewed in paper [1]. The paper [2] presents investigations on the concept described as adaptive blade twist. It is based on a representative model in which the active part of the rotor blade is simplified with a thin-walled rectangular beam that is structurally equivalent to a model rotor blade of the Bo105 with a scaling factor 2.54. Evaluation of the performance of the active twist concept with respect to rotor dynamics, stability, aerodynamics, acoustics and pilot-

ing has been done in paper [3] for the Bo105 model rotor blade. The paper [4] presents the procedure and integrated tools for aeroelastic analysis of the Active Twist Rotor (ATR) with a rectangular blade and NACA0012 airfoil. The blades are modelled as beam elements by an original finite volume formulation for the analysis of non-linear, initially curved and twisted beams subjected to large displacements and rotations. The formulation is extended to include the effects of embedded piezoelectric devices as actuators.

The models examined use simplified design parameters to reduce system complexity and to ease fabrication process. More modern blade design techniques and parameters are presented in papers [5–7] for the Advanced Active Twist Rotor (AATR). Recent achievements in helicopter and fixed wing aircraft applications of induced strain actuations are reviewed in paper [8], where two directions have been examined: distributed induced strain actuation resulting in a continuous twisting of the blade and discrete actuation of a servo aerodynamic control surface to generate localised aerodynamic forces. Most present investigations are devoted to the design of an active twist of helicopter rotor blades and only some – to the active twist optimisation. So, the capability to characterise numerically induced strain composite beam sections has been used in an optimisation problem to determine the design of the rotor blade in paper.

The objective of the present study is development of the methodology, based on the planning of experiments and response surface technique, for the optimal design of

active rotor blades using MFC actuators to obtain high piezoelectric actuation forces and displacements with the minimal actuator weight and energy applied. The structural static analysis with thermal load is carried out to characterise an active twist of the helicopter rotor blade. Design solutions for the application of active materials are studied to estimate the effectiveness.

2. Helicopter rotor blade

An investigated helicopter rotor blade (Fig 1) is equipped with NACA23012 airfoil and has a rectangular shape with active part radius 1.56 m and chord length 0.121 m. This rotor blade consists of D-spar made of unidirectional GFRP (Glas Fiber Reinforced Polymer), skin made of $+45^0/-45^0$ GFRP, foam core, MFC actuators and balance weight. MFC actuators consist of piezoceramic fibres embedded in an epoxy matrix and sandwiched between polyamide films that have attached interdigitated electrode patterns as shown in Fig 2. The direction of piezoceramic micro-fibres in MFC coincides with the direction of outside GFRP skin layers. The thickness of skin GFRP layer is 0.125 mm and thickness of MFC layer is 0.3 mm. The material properties of the rotor blade components are as follows:

- GFRP: E_x = 11.981 GPa, E_y = 11.981 GPa, E_z = 45.166 GPa, G_{xz} = 4.583 GPa, G_{yz} = 4.583 GPa, G_{xy} = 1.289 GPa, v_{yz} = 0.238, v_{xz} = 0.238, v_{xy} = 0.325, ρ = 2008 kg/m^3.
- Foam (Rohacell 51 FX): E = 0.035 GPa, G = 0.014 GPa, v = 0.25, ρ = 52 kg/m^3.
- Lead: E = 13.790 GPa, G = 2.000 GPa, v = 0.44, ρ = 11300 kg/m^3.
- MFC: E_x = 30.0 GPa, E_y = 15.5 GPa, E_z = 15.5 GPa, G_{xz} = 10.7 GPa, G_{yz} = 10.7 GPa, G_{xy} = 5.7 GPa, v_{yz} = 0.4, v_{xz} = 0.4, v_{xy} = 0.35, d_{33} = 4.18×10^{-10} m/V, d_{32} = d_{31} = −1.98×10^{-10} m/V, ρ = 4700 kg/m^3.
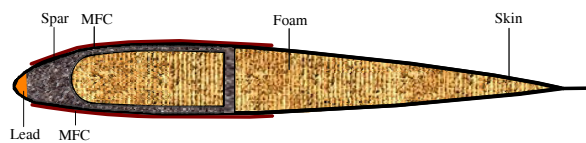

Fig 1. Cross-section of the helicopter rotor blade

3. Finite element analysis

3D finite element model of the rotor blade is produced by ANSYS (Fig 2), where rotor blade skin and spar "moustaches" are modelled by the linear layered structural shell elements SHELL99, and spar and foam – by 3D 20 node structural solid elements SOLID186. The clamped boundary conditions are applied from one end-side of the rotor blade.

Thermal strain analogy between piezoelectric strains and thermally induced strains is used to model piezoelectric effects, when piezoelectric coefficients characterizing an actuator are introduced as thermal expansion coefficients determined by the following relationship:

$$\alpha_{ij} = \frac{d_{ij}}{\Delta_{ES}},$$

where d_{ij} is the effective piezoelectric constant and Δ_{ES} is the electrode spacing (Fig 3) taken as Δ_{ES} = 0.5 mm.
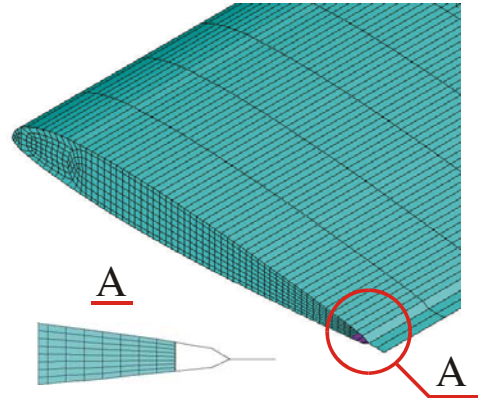

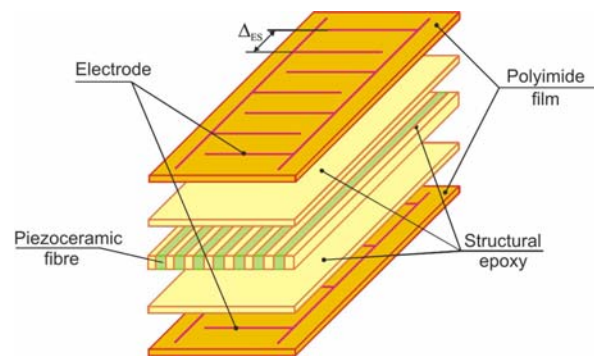**Fig 2.** Finite element model of the helicopter rotor blade

Fig 3. MFC actuator

Then steady-state thermal analysis is carried out to determine a torsion angle of the rotor blade (Fig 4), static torsion analysis – to determine the location of the elastic axis and modal analysis – to determine the first torsion eigenfrequency of the rotor blade.
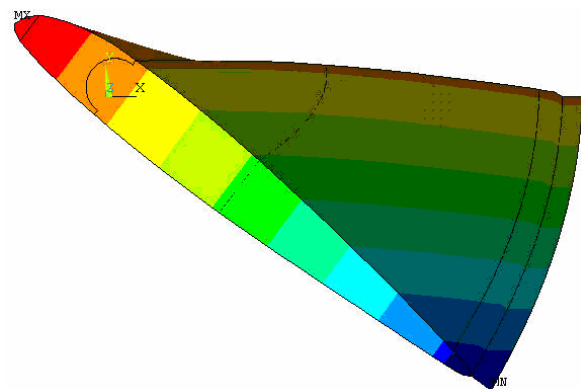

Fig 4. Torsion angle of the helicopter rotor blade

4. Parametric study

Before formulation of optimisation problem, the parametric study has been carried out with the purpose to decrease the number of design parameters (Fig 5) and by this way to increase the accuracy of obtained optimal results. In this connection the influence of possible design parameters – spar "moustaches" thickness and length, spar circular fitting, skin thickness, MFC chord-wise length, web thickness and length, web and spar "moustaches" thickness together and voltage, on the behaviour functions - torsion angle, location of centre of gravity and elastic axis, mass of cross-section, strains and first torsion eigenfrequency (Fig 6–10) were considered.
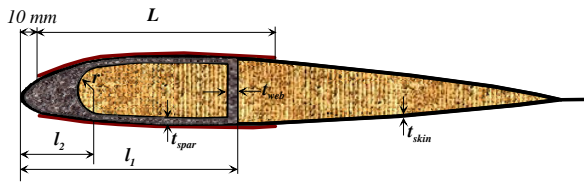

Fig 5. Design parameters of the helicopter rotor blade

Objective function: $\varphi = \varphi(x)$.
Design parameters:
$\{x\} = \{l_1, l_2, t_{skin}, t_{spar}, t_{web}, t_{spar+web}, L, V\}$,
$48 \leq l_1 \leq 56$ mm,
$16 \leq l_2 \leq 24$ mm,
$0.25 \leq t_{skin} \leq 1.25$ mm,
$0.50 \leq t_{spar} \leq 2.50$ mm,
$0.50 \leq t_{web} \leq 2.50$ mm,
$0.50 \leq t_{spar+web} \leq 2.50$ mm,
$16 \leq L \leq 100$ mm,
$100 \leq V \leq 1550$ Volt,

where φ – torsion angle (°), l_1 – web length (mm), l_2 – spar circular fitting (mm), t_{skin} – skin thickness (mm), t_{spar} – spar thickness (mm), t_{web} – web thickness (mm), $t_{spar+web}$ – spar and web thickness together (mm), L – MFC chord-wise length (mm), V – voltage (Volt), y_{cg} – location of the centre of gravity (%), y_{ea} – location of the elastic axis (%), m – mass of cross-section (kg/m), f_{T1} – first torsion eigenfrequency (Hz) and ε_{max} – admissible strains (μstrain) with the safety factor $k_s = 1.4$.
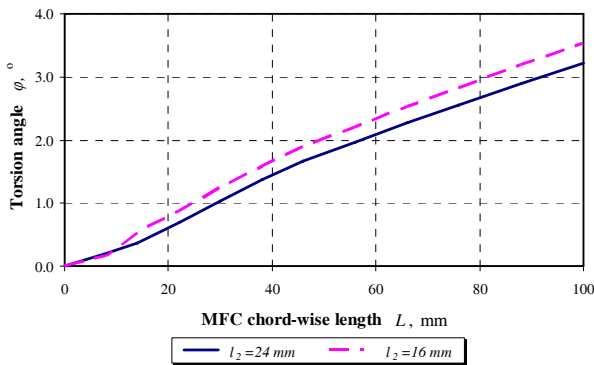

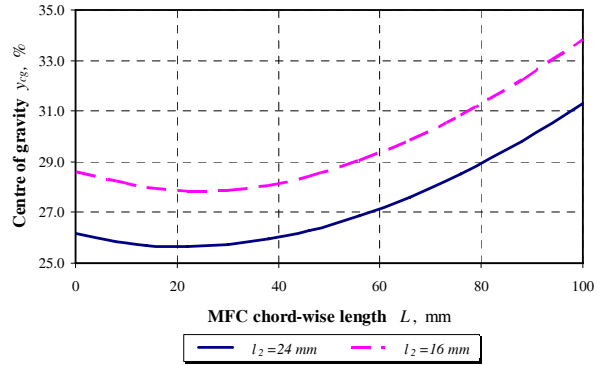**Fig 6.** Influence of MFC chord-wise length on torsion angle

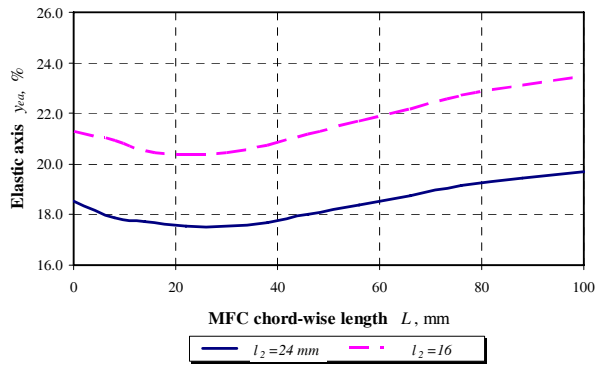**Fig 7.** Influence of MFC chord-wise length on centre of gravity

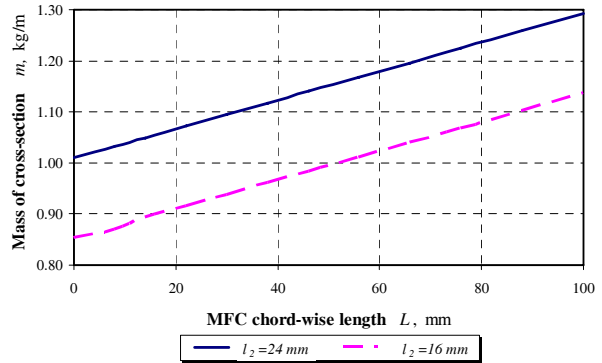**Fig 8.** Influence of MFC chord-wise length on elastic axis

Fig 9. Influence of MFC chord-wise length on mass of cross-section
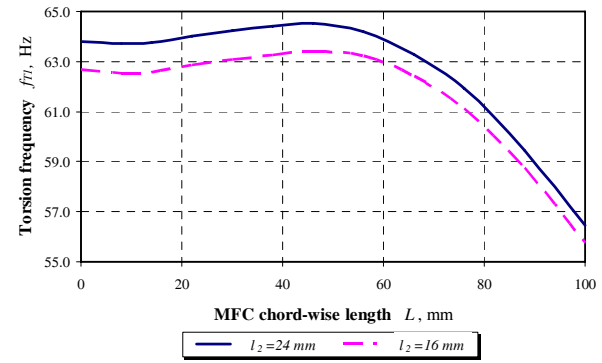

Fig 10. Influence of MFC chord-wise length on torsion frequency

The skin thickness is examined as discrete value design parameter with the step $\Delta t_{(+45/-45)} = 0.25$ mm.

The smallest influence has been shown by spar "moustaches" length, web length and web thickness. The influence on torsion angle by the spar "moustaches" thickness and web thickness together has been better than only spar "moustaches" thickness. Voltage has influence on the strain. But this influence is less than permissible. For this reason web thickness, web length, voltage and spar "moustaches" thickness have been excluded from the set of design parameters used in optimisation problem for the optimum placement of actuators in helicopter rotor blades.

The influence of spar circular fitting (Fig 11), skin thickness (Fig 12), spar and web thickness together (Fig 13) and MFC chord-wise length (Fig 6) on torsion angle illustrated lower values.
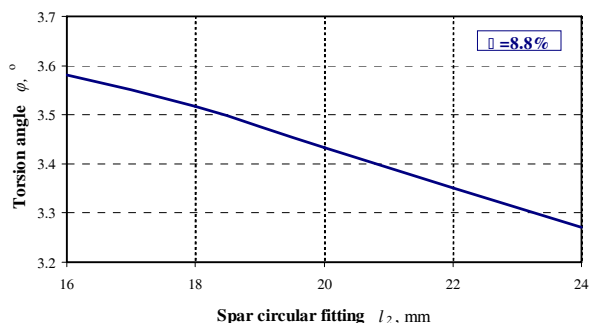

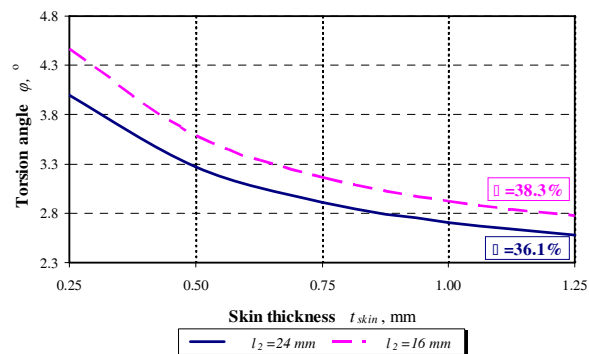**Fig 11.** Influence of spar circular fitting on torsion angle

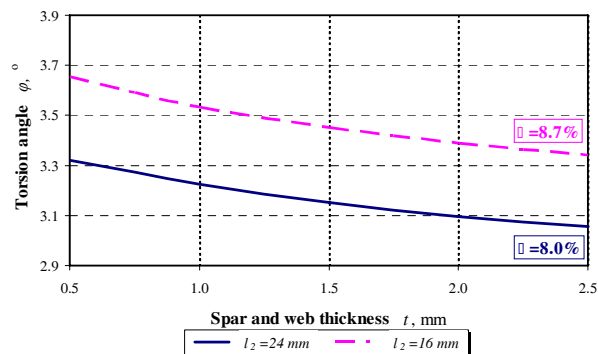**Fig 12.** Influence of skin thickness on torsion angle

Fig 13. Influence of spar and web thickness on torsion angle

5. Optimal design

Due to large dimension of the numerical problem to be solved, non-direct optimisation technique should be applied, since the application of direct minimisation algorithms and multiple finite element analysis is too expensive from the computational point of view. For this reason an optimisation methodology is developed employing the method of experimental design and response surface technique.

5.1. Formulation of optimisation problem

An optimisation problem for the optimum placement of actuators in the helicopter rotor blade (Fig 14) has been formulated on the results of parametric study and taking into account the producers requirements:

Objective function: $\varphi = \varphi(x)$.
Design parameters: $\{x\} = \{l, t_{skin}, t_{spar}, L\}$,
$16 \leq l \leq 24$ mm,
$0.25 \leq t_{skin} \leq 1.25$ mm,
$0.50 \leq t_{spar} \leq 2.50$ mm,
$16 \leq L \leq 100$ mm.

Constraints:
$22 \leq y_{cg} \leq 30$,
$10 \leq y_{cg} \leq 25$,
$10 \leq y_{cg} \leq 25$,
$m \leq 1.35$,
$f_{T1} \geq 59.15$,

where l – spar circular fitting (mm), t_{skin} – skin thickness (mm), t_{spar} – spar thickness and web thickness together (mm), L – MFC chord-wise length (mm). The length of web is 56 mm.
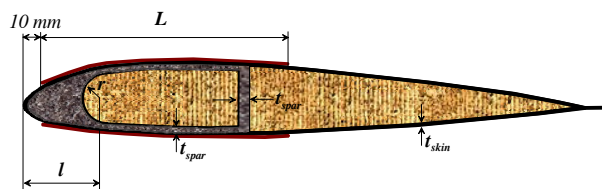

Fig 14. Design parameters

5.2. Experimental design and FEM simulations

The program EDAOpt [9] was used for the generation of experimental design. D-optimal experimental design is formulated for 4 design parameters and 30 experiments. Then in the points of plan of experiments the structural static analysis with thermal load is carried out to determine the torsion angles in the helicopter rotor blade, and modal analysis to determine its first torsion eigenfrequency. As additional parameters a location of the centre of gravity and rotor blade mass are found from the finite element model. Determination of the elastic axis location is a more complicated problem and requires solution of additional static torsion problem with two forces applied independently from both sides of sought elastic centre [10].

5.3. Response surfaces

In the present approach a form of the equation of regression is previously unknown [11]. There are two requirements for the equation of regression: accuracy and reliability. Accuracy is characterised as a minimum of standard deviation of the table data from the values given by the equation of regression. Increasing the number of terms in the equation of regression it is possible to obtain a complete agreement between the table data and values given by the equation of regression. However, it is necessary to note that prediction at the intervals between the table points can be not so good. For an improvement of prediction, it is necessary to decrease the distance between the points of experiments by increasing the number of experiments or by decreasing the domain of factors. Reliability of the equation of regression can be characterised by an affirmation that standard deviations for the table points and for any other points are approximately the same. Obviously the reliability is greater for a smaller number of terms of the equation of regression.

The equation of regression can be written in the following form:

$$y = \sum_{i=1}^{p} A_i f_i(x_j),$$

where A_i are the coefficients of the equation of regression, $f_i(x_j)$ are the functions from the bank of simple functions $\theta_1, \theta_2, \ldots \theta_m$ which are assumed as,

$$\theta_m(x_j) = \prod_{i=1}^{s} x_j^{\xi mi},$$

where ζ_{mi} is a positive or negative integer including zero. Synthesis of the equation from the bank of simple functions is carried out in two stages: selection of perspective functions from the bank and then step-by-step elimination of the selected functions.

In the first stage, all variants are tested with the least square method and the function, which leads to the minimum sum of deviations, chosen for each variant. In the second stage, the elimination is carried out using the standard deviation

$$\sigma_0 = \sqrt{\frac{S}{k-p+1}}, \quad \sigma = \sqrt{\frac{1}{k-1}\sum_{i=1}^{k}\left(y_i - \frac{1}{k}\sum_{j=1}^{k}y_j\right)^2}$$

or correlation coefficient

$$c = \left(1 - \frac{\sigma}{\sigma_0}\right) \times 100\%,$$

where k is the number of experimental points, p is the number of selected perspective functions, and S is the minimum sum of deviations. It is more convenient to characterise an accuracy of the equation of regression by the correlation coefficient (Fig 15). If insignificant functions are eliminated from the equation of regression, a reduction of the correlation coefficient is negligible. If in the equation of regression only significant functions are presented, elimination of one of them leads to important decrease of the correlation coefficient.
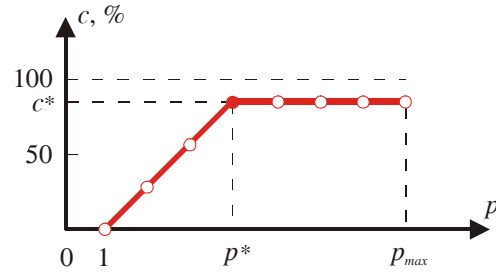

Fig 15. Diagram of elimination for the correlation coefficient

Response surfaces for all behaviour functions have been obtained with the correlation coefficients around 90 % and higher. They have been verified by the finite element solutions in the points different from the points taken in the plan of experiments. Results of verification are presented in Figs 16–18.
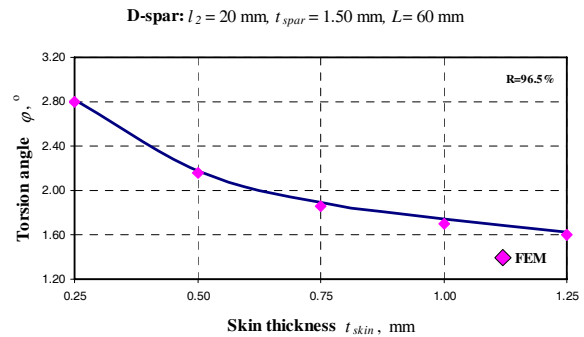

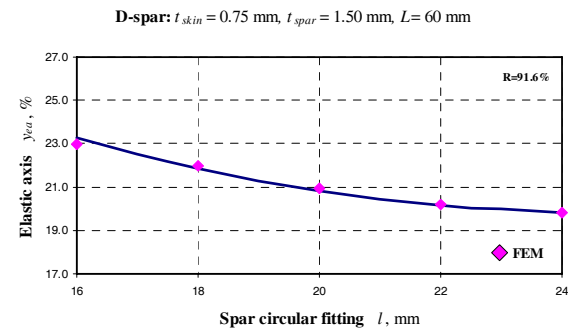**Fig 16.** Finite element verification of response surfaces

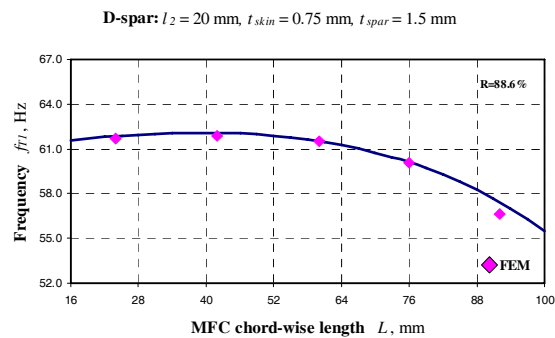**Fig 17.** Finite element verification of response surfaces

Fig 18. Finite element verification of response surfaces

5.4. Optimisation results

Non-linear global optimisation problem is executed by the Improved Multistart Random Search [12] using

response surfaces obtained. In the first stage the design problem has been solved with the purpose to obtain maximal torsion angle. Optimisation is given in Tables 1–3 together with the finite element solutions obtained in the optimal point. As it is seen the difference between finite element and response surface solutions is reasonable.

Table 1. Design parameters

	Design parameters			
	l mm	t_{skin} mm	t_{spar} mm	L mm
Response surfaces	16	0.25	1.00	89
FEM	16	0.25	1.00	88

Table 2. Constraints

	Constraints			
	y_{cg} %	y_{ea} %	m kg/m	f_{T1} Hz
Response surfaces	29.7	22.1	0.96	59.15
FEM	29.4	21.9	0.95	58.10
%	1.0	0.9	1.0	1.8

Table 3. Objective function and effectiveness

|	Objective function	Effectiveness
	φ, °	φ/L, °/m
Response surfaces	4.01	2.57
FEM	4.04	2.59
%	0.7	0.8

5.5. Parametric study

Parametric study has been carried out additionally for a designer convenience to investigate influence of different design parameters on behaviour functions.

The dependencies of torsion angle on MFC chord-wise length and spar circular fitting, first torsion frequency on MFC chord-wise length and skin thickness are given in Figs 19–20.

D-spar: t_{skin} = 0.75 mm, t_{spar} = 0.75 mm
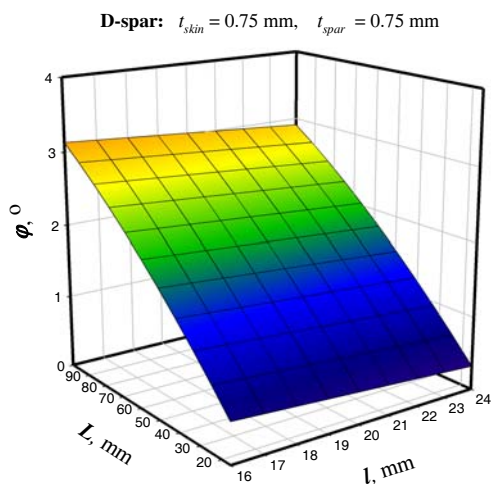
Fig 19. The dependencies of torsion angle on MFC chord-wise length and spar circular fitting

D-spar: l = 20 mm, t_{spar} = 0.75 mm
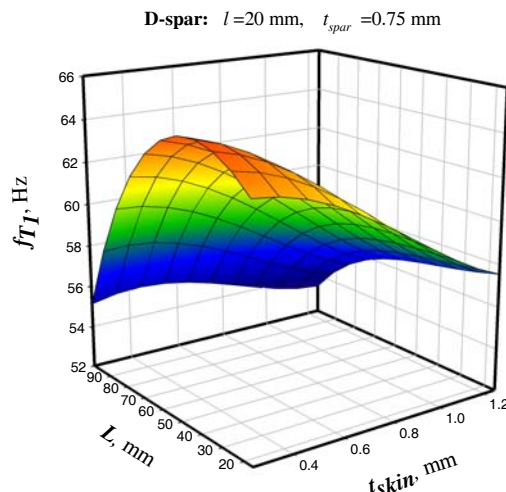
Fig 20. The dependences of first torsion frequency on MFC chord-wise length and skin thickness

The dependencies of center of gravity location on MFC chord-wise length and skin thickness are given in Fig 21.

D-spar: l = 20 mm, t_{spar} = 0.75 mm
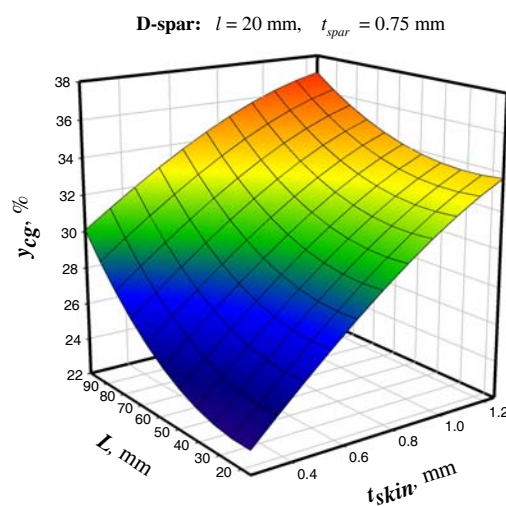
Fig 21. The dependences of gravity location on MFC chord-wise length and skin thickness

6. Conclusions

An optimisation problem for the optimum placement of actuators in the helicopter rotor blade has been formulated on the results of parametric study using the finite element method.

The methodology based on the planning of experiments and response surface technique has been developed for the optimum placement of actuators in helicopter rotor blades after parametric study. To describe the behaviour of twisted rotor blade, the finite element method has been applied in the sample points of experimental design. For this purpose the structural static analysis with thermal load using 3D finite element model has been developed by ANSYS. Minimisation problems have been solved by the Improved Mul-

tistart Random Search using the approximating functions instead of original ones.

From optimisation results it is seen that MFC chord-wise length and skin thickness have big influence on torsion angle. From approximation function it is possible to find a compromise between necessary solutions using optimal results obtained.

Acknowledgements

References

1. RODGERS, J. P.; HAGOOD, N. W. Design, manufacture and hover testing of an integral twist-actuated rotor blade. In *Proceedings of the 8th International Conference on Adaptive Structures and Technology*, 1997, p. 63–72.

2. BÜTER, A.; BREITBACH, E. Adaptive blade twist – calculations and experimental results. *Aerospace Science Technology*, 2000, 4, p. 309–319.

3. RIEMENSCHNEIDER, J.; KEYE, S.; WIERACH, P.; des ROCHETTES, H. M. Overview of the common DLR/ONERA project "Active twist blade (ATB)". In *Proceedings of the 30th European Rotorcraft Forum*, 2004, p. XX.1–XX.9.

4. GHIRINGHELLI, G. L.; MASARATI, P.; MANTEGAZZA, P. Analysis of an actively twisted rotor by multibody global modelling. *Composite Structures*, 2001, 52/1, p. 113–122.

5. SEKULA, M. K.; WILBUR, M. L.; YEAGER, W. T. Aerodynamic design study of an advanced active twist rotor. In *Proceedings of the American Helicopter Society 4th Decennial Specialists Conference on Aeromechanics*, 2004 (available at http://library-dspace.larc.nasa.gov).

6. SEKULA, M. K.; WILBUR, M. L.; YEAGER, W. T. Structural design study of an advanced active twist rotor. In *Proceedings of the 61st Annual Forum of the American Helicopter Society*, 2005 (available at http://library-dspace.larc.nasa.gov).

7. WILBUR, M. L.; SEKULA, M. K. The effect of tip geometry on active-twist rotor response. In *Proceedings of the 61st Annual Forum of the American Helicopter Society*, 2005 (available at http://library-dspace.larc.nasa.gov).

8. GIURGIUTIU, V. Active-materials induced-strain actuation for aeroelastic vibration control. *The Shock and Vibration Digest*, 2000, 32/5, p. 355–368.

9. AUZINS, J. Direct optimization of experimental designs. In *10th AIAA/ISSMO Multidisciplinary Analysis and Optimisation Conf.*, AIAA paper, No 2004–4578, 2004, p. 1–22,

10. KUHN, P. *Remarks on the elastic axis of shell wings*. National Advisory Committee for Aeronautics. Washington, Technical Notes No 562, April 1936. 12 p.

11. EGLAIS, V. Approximation of data by multi-dimensional equation of regression. *Problems of Dynamics and Strength*, 1981, Vol 39, p. 120–125.

12. JANUSEVSKIS, A.; AKINFIEV, T.; AUZINS, J. and BOYKO, A. A comparative analysis of global search procedures. In *Proceedings of the Estonian Academy of Science*, 2004, Vol 10, No 4, p. 236–250.